ELSEVIER

Chemical Engineering Science 61 (2006) 5221–5235

Chemical Engineering Science

www.elsevier.com/locate/ces

Thermocapillary motion of a fluid droplet perpendicular to two plane walls

Yu C. Chang, Huan J. Keh*

Department of Chemical Engineering, National Taiwan University, Taipei 10617, Taiwan, ROC

Received 8 February 2006; received in revised form 14 March 2006; accepted 15 March 2006
Available online 22 March 2006

Abstract

The quasisteady problem of the thermocapillary migration of a spherical fluid droplet situated at an arbitrary position between two infinite parallel plane walls is studied theoretically in the limit of negligible Marangoni and Reynolds numbers. The applied temperature gradient is constant and perpendicular to the plane walls. The presence of the plane walls causes two basic effects on the droplet velocity: first, the local temperature gradient on the droplet surface is altered by the walls, thereby speeding up or slowing down the droplet; secondly, the walls increase viscous retardation of the moving droplet. To solve the thermal and hydrodynamic governing equations, the general solutions are constructed from the fundamental solutions in both cylindrical and spherical coordinates. The boundary conditions are enforced first at the plane walls by the Hankel transforms and then on the droplet surface by a collocation technique. Numerical results for the thermocapillary migration velocity of the droplet relative to that under identical conditions in an unbounded medium are presented for various values of the relative viscosity and thermal conductivity of the droplet as well as the relative separation distances between the droplet and the confining walls. The collocation results agree well with the approximate analytical solutions obtained by using a method of reflections. The presence of the walls always reduces the droplet velocity, irrespective of the relative transport properties of the droplet or the relative droplet–wall separation distances. The boundary effect on thermocapillary migration of a droplet normal to two plane walls, which is relatively weak in comparison with the corresponding effect on sedimentation, is found to be quite significant and generally stronger than that parallel to the plane walls.

Keywords: Thermocapillary motion; Fluid sphere; Boundary effects; Parallel walls

1. Introduction

When a small droplet of one fluid is placed in a second fluid in which it is immiscible, it will migrate toward the hotter side if the surrounding fluid has a temperature gradient. This movement is owing to the temperature-induced interfacial tension gradient along the droplet surface. The thermocapillary migration of droplets was first demonstrated experimentally by Young et al. (1959). They also theoretically calculated the migration velocity of a spherical droplet of radius a placed in an infinite immiscible fluid of viscosity η_f, with a linear temperature distribution $T_\infty(\mathbf{x})$ far away from the droplet. If the droplet is sufficiently small that effects of inertia and convection of energy are negligible, its velocity $\mathbf{U}_0$ is related to the uniform temperature gradient ∇T_∞ by

$$\mathbf{U}_0 = A\nabla T_\infty, \tag{1}$$

where the thermocapillary mobility

$$A = \frac{2}{(2+k^*)(2+3\eta^*)}\left(-\frac{\partial\gamma}{\partial T}\right)\frac{a}{\eta_f}, \tag{2}$$

where $\partial\gamma/\partial T$ is the variation of the interfacial tension γ at the droplet surface with respect to the local temperature T (with a typical value of $10^{-4}\,\mathrm{N\,m^{-1}K^{-1}}$), and k^* and η^* are the ratios of thermal conductivities and viscosities, respectively, between the internal and surrounding fluids. In Eq. (2), all the physical properties are assumed to be constant except for the interfacial tension, which is assumed to vary linearly with temperature. The thermocapillary mobility of a single gas bubble can be evaluated by Eq. (2) taking the limiting values $k^*=0$ and $\eta^*=0$.

In most practical applications of thermocapillary motion, fluid droplets are not isolated and the surrounding fluid is

* Corresponding author. Fax: +886 2 23623040.
E-mail address: huan@ntu.edu.tw (H.J. Keh).

0009-2509/$ - see front matter © 2006 Elsevier Ltd. All rights reserved.
doi:10.1016/j.ces.2006.03.034

externally bounded by solid or fluid surfaces (Morton et al., 1990; Keh and Chen, 1990, 1992, 1993; Kasumi et al., 2000; Sun and Hu, 2003; Sellier, 2005). Thus, it is important to determine if the presence of neighboring boundaries significantly affects the movement of droplets. During the past quarter of century, much progress has been made in the theoretical analysis concerning the applicability of Eq. (2) for a fluid droplet in a variety of bounded systems. Through an exact representation in spherical bipolar coordinates, Meyyappan et al. (1981) and Sadhal (1983) solved the quasisteady problem of thermocapillary motion of a spherical gas bubble normal to an infinite planar solid or free fluid surface of constant temperature. Later, Meyyappan and Subramanian (1987) examined the thermocapillary motion of a gas bubble parallel to a rigid plane surface on which the far-field temperature distribution was imposed. In both cases, the bubble mobility was found to decrease monotonically relative to its isolated value given by Eq. (2) for motions close to the confining plane.

To extend the analysis by Meyyappan et al. (1981) for a gas bubble, Barton and Subramanian (1990) and Chen and Keh (1990) determined the thermocapillary migration velocity of a fluid droplet in the direction perpendicular to a nearby isothermal planar solid or free surface using spherical bipolar coordinates. Analytical solutions of this problem in asymptotic forms were obtained by using a method of reflections (Chen and Keh, 1990) and a lubrication approach (Loewenberg and Davis, 1993). In addition to the above-mentioned studies for the boundary effect on the thermocapillary motion of a fluid sphere near a planar surface, the migration of a deformable drop near another drop (Berejnov et al., 2001) or normal to an isothermal rigid plane (Ascoli and Leal, 1990) due to thermocapillarity has also been examined. The effect of a planar solid surface on fluid drops undergoing thermocapillary motion normal to it has also been investigated experimentally (Barton and Subramanian, 1991) and was found to be in good agreement with the predictions from the quasisteady analyses.

Chen et al. (1991) used a boundary collocation method to solve for the axisymmetric thermocapillary motion of a spherical drop within a long circular insulated tube. They found that the fluid sphere in the tube always moves slower than it does in an infinite medium as a result of the wall-drop thermal and hydrodynamic interactions, and the thermocapillary velocity is a monotonically decreasing function of the ratio of the sphere to the tube diameters for fixed values of k^* and η^*. At constant values of η^* and the sphere-to-tube radius ratio, the migration velocity of the drop relative to the isolated value increases as k^* decreases, because a greater portion of energy is conducted through the relatively conductive gap between the drop and the insulated tube wall which creates a larger interfacial tension gradient. Recently, the thermocapillary motion of a fluid sphere parallel to two plane walls at an arbitrary position between them has been investigated by Keh et al. (2002) using both the boundary collocation technique and the method of reflections. Exact numerical results and approximate analytical solutions of the wall-correction to Eq. (2) for the droplet mobility were presented for various values of the relative separation distances and other relevant parameters. For the case that a linear temperature profile is prescribed on the plane walls which is consistent with the far-field distribution, the migration velocity of the drop increases as k^* increases and, under the situation of large η^* and large k^*, the thermocapillary mobility of the droplet first decreases and goes through a minimum with the decrease of the droplet-to-wall distances when they are relatively large and then increases monotonically. When the gap between the droplet and the wall turns thin, the droplet can even move faster than its isolated value.

This paper is an extension of the previous work (Keh et al., 2002) to the situation of the thermocapillary motion of a spherical droplet perpendicular to two parallel plane walls at an arbitrary position between them. The effects of fluid inertia as well as thermal convection are neglected. For the case of a droplet with a relatively high thermal conductivity undergoing thermocapillary motion normal to the plane walls, the heat conduction around the droplet may generate larger temperature gradients on the droplet surface relative to those in an infinite medium. These gradients enhance the thermocapillary migration velocity, although their action will be retarded by the viscous interaction of the migrating droplet with the walls. The effects of the thermal enhancement and the hydrodynamic retardation both increase as the ratios of the radius of the droplet to its distances from the walls increase. Determining which effect is overriding at small droplet–wall gap widths is a main target of this study. Because the governing equations and boundary conditions concerning the general problem of thermocapillary motion of a droplet at an arbitrary position between two parallel plane walls in an arbitrary direction are linear, its solution can be obtained as a superposition of the solutions for its two subproblems: motion parallel to the plane walls, which was previously examined (Keh et al., 2002), and motion normal to the confining walls, which is considered in this work. Unfortunately, with only one exception (Barton and Subramanian, 1991), no experimental data available in the literature involve the thermocapillary migration velocity of a fluid sphere as a function of its position between two parallel plane walls or near a single plane wall for a comparison with the theoretical predictions.

2. Analysis

We consider the quasisteady thermocapillary migration of a spherical fluid droplet of radius a in an immiscible fluid perpendicular to two infinite plane walls whose distances from the center of the droplet are b and c, as shown in Fig. 1. Here (ρ, ϕ, z) and (r, θ, ϕ) denote the circular cylindrical and spherical coordinate systems, respectively, and the origin of coordinates is chosen at the droplet center. A linear temperature field $T_\infty(z)$ with a uniform thermal gradient $E_\infty \mathbf{e}_z$ (equal to ∇T_∞) is imposed in the external fluid far removed from the droplet, where $\mathbf{e}_z$ is the unit vector in the z direction and, for convenience, E_∞ is taken to be positive. The capillary number $\eta_f U_0/\gamma$ (where $U_0 = |\mathbf{U}_0|$ is given by Eqs. (1) and (2)) is assumed to be sufficiently small so that interfacial tension maintains the spherical shape of the droplet during the confined thermocapillary migration. Gravitational and natural-convection effects are ignored. The purpose is to obtain the

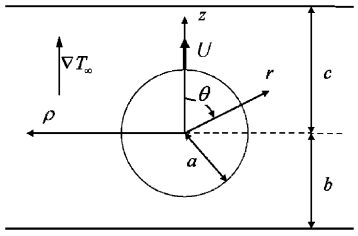

Fig. 1. Geometrical sketch for the thermocapillary motion of a spherical droplet perpendicular to two plane walls at an arbitrary position between them.

correction to Eq. (2) for the droplet mobility due to the presence of the plane walls.

To determine the thermocapillary migration velocity of the droplet, it is necessary to ascertain the temperature and velocity distributions in both internal and external fluid phases.

2.1. Temperature distribution

For the heat transfer in a system of thermocapillary motion, the Marangoni number (Peclet number) can be assumed to be small. Hence, the energy equations governing the temperature distribution are

$$\nabla^2 T = 0 \quad (r \geqslant a) \tag{3a}$$

for the external fluid and

$$\nabla^2 T_1 = 0 \quad (r \leqslant a) \tag{3b}$$

for the fluid inside the droplet.

The boundary conditions at the droplet surface require that the temperature and the normal component of heat flux be continuous, namely,

$$r = a\text{: } T = T_1, \tag{4a}$$

$$k\frac{\partial T}{\partial r} = k_1 \frac{\partial T_1}{\partial r}. \tag{4b}$$

Here k and k_1 are the thermal conductivities of the external and internal fluids, respectively. Since the temperature field far away from the droplet approaches the undisturbed values, we can write

$$z = c\text{: } T = T_0 + E_\infty c, \tag{5}$$

$$z = -b\text{: } T = T_0 - E_\infty b, \tag{6}$$

$$\rho \to \infty\text{: } T \to T_\infty = T_0 + E_\infty z, \tag{7}$$

where T_0 is the undisturbed temperature at the droplet center. The temperatures at the two parallel plane walls have been set equal to different constants to allow a uniform thermal gradient in their normal direction far from the droplet.

The external temperature distribution, which is governed by the Laplace equation, can be expressed as the superposition

$$T = T_0 + E_\infty z + T_w + T_p. \tag{8}$$

Here, T_w is a separable solution of Eq. (3a) in cylindrical coordinates that represents the disturbance produced by the plane walls and is given by a Fourier–Bessel integral

$$T_w = E_\infty \int_0^\infty [X(\omega)\mathrm{e}^{\omega z} + Y(\omega)\mathrm{e}^{-\omega z}]\omega J_0(\omega\rho)\,\mathrm{d}\omega, \tag{9}$$

where J_n is the Bessel function of the first kind of order n and $X(\omega)$ and $Y(\omega)$ are unknown functions of the separation variable ω. The last term on the right-hand side of Eq. (8), T_p, is a separable solution of Eq. (3a) in spherical coordinates representing the disturbance generated by the droplet and is given by an infinite series in harmonics,

$$T_p = E_\infty \sum_{m=0}^{\infty} R_m r^{-m-1} P_m(\cos\,\theta), \tag{10}$$

where P_m is the Legendre polynomial of order m and R_m are unknown constants. Note that a solution for T of the form given by Eqs. (8)–(10) immediately satisfies the boundary condition (7) at infinity. Since the temperature is finite for any position in the interior of the droplet, the solution to Eq. (3b) can be written as

$$T_1 = T_0 + E_\infty \sum_{m=0}^{\infty} \overline{R}_m r^m P_m(\cos\theta), \tag{11}$$

where $\overline{R}_m$ are unknown constants.

Substituting the temperature distribution T given by Eqs. (8)–(10) into the boundary conditions (5) and (6) and applying the Hankel transform on the variable ρ lead to a solution for the functions $X(\omega)$ and $Y(\omega)$ in terms of the coefficients R_m. After the substitution of this solution into Eqs. (8)–(10), T can be expressed as

$$T = T_0 + E_\infty z + E_\infty \sum_{m=0}^{\infty} R_m \delta_m^{(1)}(r,\theta), \tag{12}$$

where the function $\delta_m^{(1)}(r,\theta)$ is defined by Eq. (B.1) in Appendix B (in which the integration must be performed numerically). Applying the boundary conditions given by Eq. (4) to Eqs. (11) and (12) yields

$$\sum_{m=0}^{\infty} [R_m \delta_m^{(1)}(a,\theta) - \overline{R}_m a^m P_m(\cos\theta)] = -a\cos\theta, \tag{13a}$$

$$\sum_{m=0}^{\infty} [R_m \delta_m^{(2)}(a,\theta) - \overline{R}_m k^* m a^{m-1} P_m(\cos\theta)] = -\cos\theta, \tag{13b}$$

where the definition of functions $\delta_m^{(2)}(r,\theta)$ is given by Eq. (B.2) and $k^* = k_1/k$.

To satisfy the conditions in Eq. (13) exactly along the entire surface of the droplet would require the solution of the entire infinite array of unknown constants R_m and $\overline{R}_m$. However, the collocation technique (Ganatos et al., 1980; Keh et al., 2002) enforces the boundary conditions at a finite number of discrete points on the semicircular longitudinal generating arc of the droplet (from $\theta = 0$ to π) and truncates the infinite series in Eqs. (11) and (12) into finite ones. If the spherical boundary is approximated by satisfying the conditions (4a) and (4b) at

M discrete points on the generating arc, the infinite series in Eqs. (11) and (12) are truncated after M terms, resulting in a system of $2M$ simultaneous linear algebraic equations in the truncated form of Eq. (13). This matrix equation can be numerically solved to yield the $2M$ unknown constants R_m and $\overline{R}_m$ required in the truncated form of Eqs. (11) and (12) for the temperature distribution. The accuracy of the boundary-collocation/truncation technique can be improved to any degree by taking a sufficiently large value of M. Naturally, as $M \to \infty$ the truncation error vanishes and the overall accuracy of the solution depends only on the numerical integration required in evaluating the functions $\delta_m^{(1)}$ and $\delta_m^{(2)}$ in Eq. (13).

2.2. Fluid velocity distribution

Having obtained the solution for the external temperature distribution on the droplet surface which drives the thermocapillary migration, we can now proceed to find the flow field. Owing to the low Reynolds number encountered in thermocapillary motions, the fluid motion is governed by the fourth-order differential equations for viscous axisymmetric creeping flows,

$$E^2(E^2\Psi) = 0 \quad (r \geqslant a), \tag{14a}$$

$$E^2(E^2\Psi_1) = 0 \quad (r \leqslant a), \tag{14b}$$

where Ψ_1 and Ψ are the Stokes stream functions for the flow inside the droplet and for the external flow, respectively, which are related to the components of corresponding fluid velocity in cylindrical coordinates by ($v_\phi = v_{1\phi} = 0$)

$$v_\rho = \frac{1}{\rho}\frac{\partial\Psi}{\partial z}, \quad v_{1\rho} = \frac{1}{\rho}\frac{\partial\Psi_1}{\partial z}, \tag{15a,b}$$

$$v_z = -\frac{1}{\rho}\frac{\partial\Psi}{\partial\rho}, \quad v_{1z} = -\frac{1}{\rho}\frac{\partial\Psi_1}{\partial\rho}, \tag{15c,d}$$

and the Stokes operator E^2 has the form

$$E^2 = \rho\frac{\partial}{\partial\rho}\left(\frac{1}{\rho}\frac{\partial}{\partial\rho}\right) + \frac{\partial^2}{\partial z^2}. \tag{16}$$

The boundary conditions for the fluid velocities at the droplet surface (Young et al., 1959; Anderson, 1985), on the plane walls, and far from the droplet are

$$r = a: \ v_\rho = v_{1\rho}, \tag{17a}$$

$$v_z = v_{1z}, \tag{17b}$$

$$v_\rho \tan\theta + v_z = U, \tag{17c}$$

$$\tau_{r\theta} - \tau_{1r\theta} = -\frac{\partial\gamma}{\partial T}\frac{\partial T}{r\partial\theta}, \tag{17d}$$

$$z = c, -b: \ v_\rho = v_z = 0, \tag{18}$$

$$\rho \to \infty: \ v_\rho = v_z = 0. \tag{19}$$

Here, $\tau_{r\theta}$ and $\tau_{1r\theta}$ are the viscous shear stresses for the external flow and the flow inside the droplet, respectively, and U is the thermocapillary migration velocity of the droplet to be determined.

To solve the external flow field, we express its stream function in the form (Ganatos et al., 1980)

$$\Psi = \Psi_w + \Psi_p. \tag{20}$$

Here Ψ_w is a separable solution of Eq. (14a) in cylindrical coordinates that represents the disturbance produced by the plane walls and is given by a Fourier–Bessel integral

$$\Psi_w = \int_0^\infty [A(\omega)e^{\omega z} + B(\omega)e^{-\omega z} + C(\omega)\omega z e^{\omega z} + D(\omega)\omega z e^{-\omega z}]\rho J_1(\omega\rho)\,d\omega, \tag{21}$$

where $A(\omega)$, $B(\omega)$, $C(\omega)$, and $D(\omega)$ are unknown functions of the separation variable ω. The second part of Ψ, denoted by Ψ_p, is a separable solution of Eq. (14a) in spherical coordinates representing the disturbance generated by the droplet and is given by

$$\Psi_p = \sum_{n=2}^{\infty}(B_n r^{-n+1} + D_n r^{-n+3})G_n^{-1/2}(\cos\theta), \tag{22}$$

where $G_n^{-1/2}$ is the Gegenbauer polynomial of the first kind of order n and degree $-\frac{1}{2}$; B_n and D_n are unknown constants. Note that the boundary condition in Eq. (19) is immediately satisfied by a solution of the form given by Eqs. (20)–(22).

The general solution to Eq. (14b) for the internal flow field can be expressed as

$$\Psi_1 = \sum_{n=2}^{\infty}(A_n r^n + C_n r^{n+2})G_n^{-1/2}(\cos\theta), \tag{23}$$

or

$$v_{1\rho} = \sum_{n=2}^{\infty}[A_n\alpha_{1n}^{(1)}(r,\theta) + C_n\alpha_{2n}^{(1)}(r,\theta)], \tag{24a}$$

$$v_{1z} = \sum_{n=2}^{\infty}[A_n\alpha_{1n}^{(2)}(r,\theta) + C_n\alpha_{2n}^{(2)}(r,\theta)], \tag{24b}$$

where the definitions of the functions $\alpha_{in}^{(j)}(r,\theta)$ for i and j equal to 1 or 2 are given by Eqs. (B.4) and (B.5) in Appendix B, and A_n and C_n are unknown constants. A solution of this form satisfies the requirement that the velocity is finite for any position within the droplet.

Substituting the stream function Ψ given by Eqs. (20)–(22) into the boundary conditions in Eq. (18) and applying the Hankel transform on the variable ρ lead to a solution for the functions $A(\omega)$, $B(\omega)$, $C(\omega)$, and $D(\omega)$ in terms of the coefficients B_n and D_n. After the substitution of this solution into Eqs. (20)–(22), the fluid velocity components can be expressed as

$$v_\rho = \sum_{n=2}^{\infty}[B_n\gamma_{1n}^{(1)}(r,\theta) + D_n\gamma_{2n}^{(1)}(r,\theta)], \tag{25a}$$

$$v_z = \sum_{n=2}^{\infty}[B_n\gamma_{1n}^{(2)}(r,\theta) + D_n\gamma_{2n}^{(2)}(r,\theta)], \tag{25b}$$

where the definitions of the functions $\gamma_{in}^{(j)}(r,\theta)$ for i and j equal to 1 or 2 are given by Eqs. (B.6) and (B.7) (in integral forms which must be evaluated numerically).

The only boundary conditions that remain to be satisfied are those on the droplet surface. Substituting Eqs. (24) and (25) into Eq. (17), one obtains

$$\sum_{n=2}^{\infty}[B_n\gamma_{1n}^{(1)}(a,\theta)+D_n\gamma_{2n}^{(1)}(a,\theta) - A_n\alpha_{1n}^{(1)}(a,\theta)-C_n\alpha_{2n}^{(1)}(a,\theta)]=0, \tag{26a}$$

$$\sum_{n=2}^{\infty}[B_n\gamma_{1n}^{(2)}(a,\theta)+D_n\gamma_{2n}^{(2)}(a,\theta) - A_n\alpha_{1n}^{(2)}(a,\theta)-C_n\alpha_{2n}^{(2)}(a,\theta)]=0, \tag{26b}$$

$$\sum_{n=2}^{\infty}\left\{B_n[\gamma_{1n}^{(1)}(a,\theta)\tan\theta+\gamma_{1n}^{(2)}(a,\theta)] +D_n[\gamma_{2n}^{(1)}(a,\theta)\tan\theta+\gamma_{2n}^{(2)}(a,\theta)]\right\}=U, \tag{26c}$$

$$\sum_{n=2}^{\infty}[B_n\gamma_{1n}^{*}(a,\theta)+D_n\gamma_{2n}^{*}(a,\theta)-\eta^{*}A_n\alpha_{1n}^{*}(a,\theta) -\eta^{*}C_n\alpha_{2n}^{*}(a,\theta)] =-\left(\frac{\partial\gamma}{\partial T}\right)\frac{E_\infty}{\eta_f}\left[\sum_{m=0}^{\infty}R_m\delta_m^{(3)}(a,\theta)-\sin\theta\right], \tag{26d}$$

where the functions $\delta_m^{(3)}(r,\theta)$, $\alpha_{in}^{*}(r,\theta)$, and $\gamma_{in}^{*}(r,\theta)$ for $i=1$ or 2 are defined by Eqs. (B.3), (B.16), and (B.17) (in which the integration must be performed numerically). The first M coefficients R_m have been determined through the procedure given in the previous subsection.

Equation (26) can be satisfied by utilizing the collocation technique presented for the solution of the temperature field. Along a longitudinal generating arc at the droplet surface, Eq. (26) is applied at N discrete points (values of θ between 0 and π) and the infinite series in Eqs. (23)–(25) are truncated after N terms. This generates a set of $4N$ linear algebraic equations for the $4N$ unknown constants A_n, C_n, B_n, and D_n. The fluid velocity field is completely obtained once these coefficients are solved for a sufficiently large number of N.

2.3. Derivation of the droplet velocity

The hydrodynamic drag force acting on the droplet can be determined from (Happel and Brenner, 1983)

$$F=4\pi\eta_f D_2. \tag{27}$$

This expression shows that only the lowest-order coefficient D_2 contributes to the drag force exerted on the droplet by the surrounding fluid.

Since the droplet is freely suspended in the surrounding fluid, the net force acting on the droplet must vanish. Applying this constraint to Eq. (27), one has

$$D_2=0. \tag{28}$$

To determine the thermocapillary migration velocity U of the droplet, Eq. (28) and the $4N$ algebraic equations resulting from Eq. (26) are to be solved simultaneously. Note that, similar to the thermocapillary migration velocity of an isolated droplet given by Eqs. (1) and (2), the value of U is proportional to the quantity $(-\partial\gamma/\partial T)(a/\eta_f)$ and dependent on the dimensionless parameters k^* and η^* (in addition to the length ratios among a, b, and c).

If the droplet velocity in Eq. (17c) is disabled (i.e., $U=0$ is set), then the force obtained from Eq. (27) can be taken as the thermocapillary force exerted on the droplet near the walls due to the prescribed temperature gradient ∇T_∞. This force can be expressed as

$$F=6\pi\eta_f a U_0\frac{3\eta^*+2}{3\eta^*+3}F^*, \tag{29}$$

where U_0 is a characteristic velocity (the thermocapillary migration velocity of the droplet in the absence of the plane walls) given by Eqs. (1) and (2) and F^* is the normalized magnitude of the thermocapillary force. The value of F^* also equals f^*U/U_0, where f^* is the dimensionless Stokes resistance coefficient of the droplet migrating normal to the two plane walls driven by a body force in the absence of the temperature gradient (Chang and Keh, 2006) and U is the wall-corrected thermocapillary migration velocity of the droplet obtained from Eq. (28).

3. Results and discussion

The numerical results for the thermocapillary motion of a fluid sphere perpendicular to two plane walls at an arbitrary position between them, obtained by using the boundary-collocation method described in the previous section, is presented in this section. The system of linear algebraic equations to be solved for the coefficients R_m and $\overline{R}_m$ is constructed from Eq. (13), while that for A_n, B_n, C_n, and D_n is composed of Eq. (26). All the numerical integrations to evaluate the functions $\delta_m^{(j)}$, $\gamma_{in}^{(j)}$, and γ_{in}^{*} were done by the 180-point Gauss–Laguerre quadrature.

When selecting the points along the half-circular generating arc of the spherical droplet where the boundary conditions are to be exactly satisfied, the first points that should be chosen are $\theta=0$ and π, since these stagnation points control the gaps between the droplet and the plane walls. In addition, the point $\theta=\pi/2$ which defines the projected area of the droplet normal to the direction of migration is also important. However, an examination of the systems of linear algebraic equations (13) and (26) shows that the matrix equations become singular if these points are used. To overcome this difficulty, these points are replaced by four closely adjacent basic points, i.e., $\theta=\delta$, $\pi/2-\delta$, $\pi/2+\delta$, and $\pi-\delta$ (Ganatos et al., 1980). Additional points along the generating arc are selected as mirror-image pairs about the plane $\theta=\pi/2$ to divide the two quarter-circular

Table 1
Normalized thermocapillary migration velocity of a spherical droplet perpendicular to a single plane wall computed from the boundary-collocation solution and the asymptotic method-of-reflection solution

a/b	U/U_0			
	$\eta^*=0$		$\eta^*=10$	
	Collocation solution	Asymptotic solution	Collocation solution	Asymptotic solution
$k^*=0$				
0.2	0.99499	0.99499	0.99504	0.99504
0.4	0.95915	0.95918	0.96044	0.96043
0.6	0.85472	0.85572	0.86195	0.86327
0.8	0.61344	0.62872	0.63758	0.66407
0.9	0.38987	0.44147	0.42868	0.51865
0.95	0.22749	0.32260	0.27182	0.43643
0.99	0.05363	0.21314	0.08375	0.36798
0.995	0.02755		0.04906	
0.999	0.00566		0.01362	
$k^*=1$				
0.2	0.99599	0.99599	0.99604	0.99604
0.4	0.96709	0.96714	0.96850	0.96851
0.6	0.88066	0.88216	0.88930	0.89089
0.8	0.66618	0.68870	0.69875	0.72931
0.9	0.44618	0.52340	0.50277	0.60953
0.95	0.27159	0.41625	0.33921	0.54121
0.99	0.06771	0.31626	0.11562	0.48399
0.995	0.03518		0.06951	
0.999	0.00731		0.01995	
$k^*=10$				
0.2	0.99749	0.99749	0.99755	0.99755
0.4	0.97919	0.97925	0.98074	0.98077
0.6	0.92203	0.92412	0.93252	0.93440
0.8	0.76349	0.79444	0.81001	0.84282
0.9	0.57218	0.68170	0.66707	0.78246
0.95	0.39246	0.60830	0.52560	0.75266
0.99	0.12590	0.53977	0.25895	0.73145
0.995	0.07116		0.17852	
0.999	0.01683		0.06428	

arcs of the droplet into equal segments. The optimum value of δ in this work is found to be 0.01°, with which the numerical results of the droplet velocity converge satisfactorily.

3.1. Motion normal to a single plane wall

Numerical solutions for the thermocapillary migration velocity of a spherical droplet near a single plane wall (i.e., with $c \to \infty$) caused by a temperature gradient in the normal direction are presented in Table 1 for various values of the parameters k^*, η^*, and a/b at the quasisteady state using the boundary-collocation method. The velocity for the thermocapillary motion of an identical droplet in an infinite fluid, $U_0 = AE_\infty$ given by Eqs. (1) and (2), is used to normalize the boundary-corrected values. All of the results obtained under this collocation scheme converge satisfactorily to at least the significant figures shown in the table. The accuracy and convergence behavior of the truncation technique is principally a function of the ratio a/b. For general cases with $a/b \leqslant 0.9$, the numbers of collocation points $M = 26$ and $N = 26$ can lead to these satisfactory results. For the most difficult case with $a/b = 0.999$, the numbers $M = 200$ and $N = 200$ are sufficiently large to achieve this convergence.

In Appendix A, an approximate analytical solution for the same thermocapillary motion as that considered here is also obtained by using a method of reflections. The droplet velocity normal to an isothermal plane wall is given by Eq. (A.11), which is a power series expansion in λ ($=a/b$). The values of the wall-corrected normalized thermocapillary mobility calculated from this asymptotic solution, with the $O(\lambda^9)$ term neglected, are also listed in Table 1 for comparison. It can be seen that the asymptotic formula of Eq. (A.11) from the method of reflections for U/U_0 agrees very well with the collocation results as long as $\lambda \leqslant 0.8$; the errors in all cases are less than 4.4%. However, accuracy of Eq. (A.11) begins to deteriorate, as expected, when the relative spacing between the droplet and the plane wall becomes small (say, $\lambda \geqslant 0.9$). In general, the formula of Eq. (A.11) overestimates the thermocapillary migration velocity of the droplet.

Through the use of spherical bipolar coordinates, Chen and Keh (1990) obtained some semianalytical–seminumerical solutions for the normalized themocapillary velocity U/U_0 of a spherical droplet perpendicular to an isothermal plane wall. In general, these solutions are in agreement with our results given in Table 2. A detailed comparison shows that our collocation solutions agree better with the method-of-reflection solution given by Eq. (A.11) than the bipolar-coordinate solutions do for all values of $a/b \leqslant 0.6$.

The collocation solutions for the normalized velocity U/U_0 of a spherical droplet undergoing thermocapillary motion perpendicular to a plane wall as functions of a/b are depicted in Fig. 2 for various values of k^* and η^*. For any set of fixed values of k^* and η^*, U/U_0 decreases monotonically with an increase in a/b and approaches zero in the limit. As expected, the droplet migrates with the velocity that would exist in the absence of the wall as a/b goes to 0. However, the boundary effect of the plane wall on thermocapillary motion can be quite significant when a/b becomes greater. The wall-corrected normalized thermocapillary mobility U/U_0 of the droplet increases with an increase in k^*, keeping the other factors η^* and a/b unchanged. This increase in the droplet mobility in general becomes more pronounced as a/b increases. This behavior is expected knowing that the local temperature gradients along the droplet surface near an isothermal plane wall with a perpendicularly imposed thermal gradient increase as k^* increases (the tangential temperature gradient at the droplet surface on the near side to the plane wall is depressed compared with that on the far side, as can be seen in the analysis given by Keh and Lien (1991) or in Appendix B). On the other hand, the wall-corrected normalized thermocapillary mobility of the droplet increases with an increase in η^* for any given values of k^* and a/b, in agreement with the prediction from the method-of-reflection solution given by Eq. (A.7) or (A.11). For the particular case of $k^* = 1$, the effect of thermal interaction between the droplet and the wall disappears, and the relative thermocapillary mobility of the droplet decreases with a/b solely owing to the hydrodynamic resistance exerted by the plane wall.

Table 2
Normalized thermocapillary migration velocity of a spherical droplet perpendicular to two equally distant plane walls (with $c = b$) computed from the boundary-collocation solution and the asymptotic method-of-reflection solution

a/b	U/U_0			
	$\eta^* = 0$		$\eta^* = 10$	
	Collocation solution	Asymptotic solution	Collocation solution	Asymptotic solution
$k^* = 0$				
0.2	0.99129	0.99129	0.99142	0.99142
0.4	0.93131	0.93150	0.93493	0.93566
0.6	0.77504	0.77958	0.79601	0.80970
0.8	0.48611	0.52723	0.54356	0.64206
0.9	0.27753	0.37874	0.34891	0.56972
0.95	0.15089	0.30544	0.21631	0.54333
0.99	0.03315	0.24989	0.06577	0.52889
0.995	0.01686		0.03853	
0.999	0.00343		0.01072	
$k^* = 1$				
0.2	0.99367	0.99367	0.99380	0.99381
0.4	0.94930	0.94939	0.95301	0.95363
0.6	0.82684	0.82920	0.84957	0.86140
0.8	0.57064	0.59513	0.64031	0.73084
0.9	0.35466	0.42353	0.45080	0.66808
0.95	0.20562	0.32202	0.30152	0.64248
0.99	0.04901	0.23272	0.10273	0.62657
0.995	0.02533		0.06188	
0.999	0.00525		0.01782	
$k^* = 10$				
0.2	0.99727	0.99727	0.99740	0.99740
0.4	0.97759	0.97761	0.98144	0.98198
0.6	0.91819	0.91941	0.94386	0.95475
0.8	0.76378	0.78575	0.86043	0.95278
0.9	0.58477	0.67070	0.75386	0.99561
0.95	0.41436	0.59584	0.62865	1.04015
0.99	0.14318	0.52582	0.33664	1.09193
0.995	0.08273		0.23627	
0.999	0.02014		0.08673	

In general, our theoretical predictions agree with the available experimental results (Barton and Subramanian, 1991).

For the creeping motion of a spherical droplet on which a constant body force $F\mathbf{e}_z$ (e.g., a gravitational field) is exerted normal to an infinite plane wall, the numerical result of the droplet velocity has recently been obtained by using the boundary-collocation technique (Chang and Keh, 2006). A comparison of the boundary effects on the translation of the fluid sphere under gravity (in which $U_0 = (F/6\pi\eta_f a)(3\eta^* + 3)/(3\eta^* + 2)$) and on the thermocapillary migration is given in Fig. 3. Obviously, the wall effect on thermocapillary motion is much weaker than that on a sedimenting or buoyantly rising droplet (also see the discussion after Eq. (A.7) in Appendix A). Note that the wall effect on the droplet motion in a gravitational field is stronger when the value of η^* becomes larger, which is opposite to that which would occur if the droplet migrates near a plane wall due to thermocapillarity.

Because the governing equations and boundary conditions concerning the general problem of thermocapillary motion of a droplet in an arbitrary direction near a plane wall are linear, the solution can be obtained as a superposition of the solutions for its two subproblems: motion perpendicular to the plane, which is examined in this paper, and motion parallel to the plane. The collocation solutions for the thermocapillary motion of a spherical droplet parallel to a plane wall have

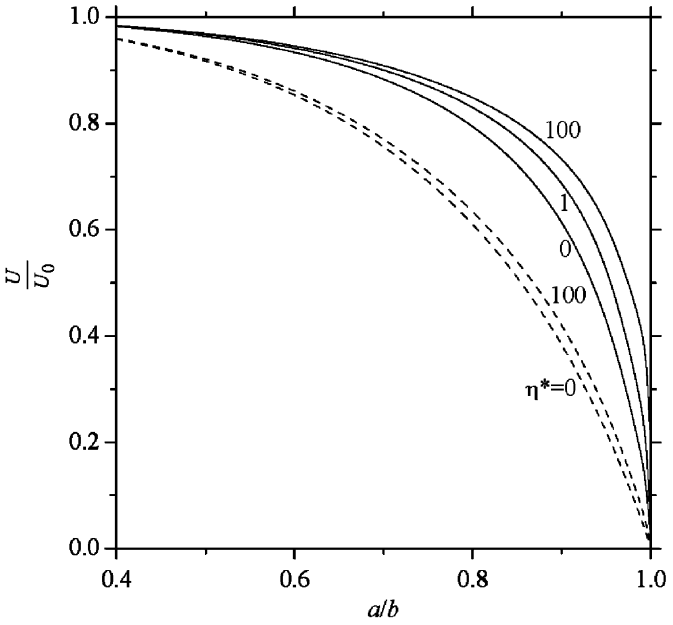

Fig. 2. Plots of the normalized thermocapillary mobility U/U_0 of a spherical droplet migrating perpendicular to a plane wall versus the separation parameter a/b for various values of η^*. The solid curves represent the case of $k^* = 100$ and the dashed curves denote the case of $k^* = 0$.

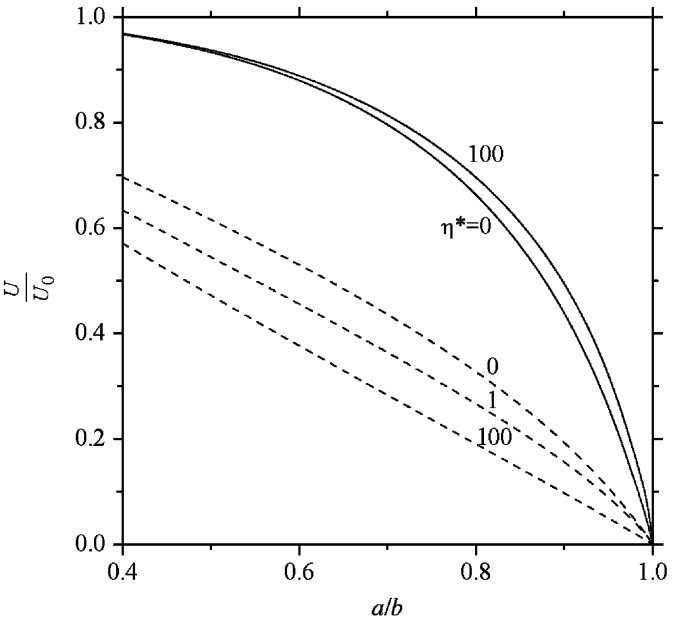

Fig. 3. Plots of the normalized thermocapillary mobility (solid curves, with $k^* = 1$) and sedimenting mobility (dashed curves) of a spherical droplet migrating perpendicular to a plane wall versus the separation parameter a/b for different values of η^*.

already been obtained by Keh et al. (2002). It was found that, when the wall is prescribed with a linear temperature profile consistent with the far-field temperature distribution, the wall-corrected normalized thermocapillary migration velocity of the droplet also increases with an increase in k^*, keeping η^* and a/b unchanged. A comparison between Table 1 of Keh et al. and our Table 1 indicates that the plane wall in general exerts the most influence on the droplet when thermocapillary motion occurs normal to it, and the least in the case of thermocapillary motion parallel to it. Evidently, the direction of motion of a droplet near a plane wall is different from that of the prescribed thermal gradient, except when it is oriented parallel or perpendicular to the plane wall.

3.2. Motion perpendicular to two plane walls

Numerical results of the normalized thermocapillary migration velocity U/U_0 of a spherical droplet perpendicular to two parallel plane walls with equal distances from the droplet ($c=b$) are presented in Table 2 for various values of the parameters k^*, η^*, and a/b using the boundary-collocation method. The corresponding method-of-reflection solutions, given by Eq. (A.20) in Appendix A as a power series expansion in λ ($=a/b$) correct to $O(\lambda^8)$, are also listed in this table for comparison. Similar to the case of migration of a droplet normal to a single plane wall considered in the previous subsection, the approximate analytical formula (A.20) agrees quite well with the exact results as long as $\lambda \leqslant 0.6$, but can have significant errors when $\lambda \geqslant 0.8$. Formula (A.20) always overestimates the thermocapillary migration velocity of the droplet. When all the values of k^*, η^*, and $a.b$ are sufficiently large (e.g., $k^*=\eta^*=10$ and $a/b \geqslant 0.95$), Eq. (A.20) accurate to $O(\lambda^8)$ predicts that the droplet can even move faster than it would as a/b goes to 0. However, the collocation solutions show that U/U_0 is always a monotonic decreasing function of a/b for any combination of constant values of k^* and η^*. This result indicates that the effect of hydrodynamic retardation, rather than that of the possible thermal enhancement, is overriding for the thermocapillary motion of a fluid sphere normal to two parallel plane walls. A comparison between Table 2 for the case of a slit and Table 1 for the case of a single normal plane indicates that the assumption that the boundary effect for two walls can be obtained by simple addition of single-wall effects leads to a greater correction to thermocapillary motion for any given value of a/b.

The collocation results for the normalized thermocapillary mobility U/U_0 of a spherical droplet locating midway between two parallel plane walls (with $c=b$) caused by a perpendicular thermal gradient are plotted in Fig. 4 as functions of a/b for several values of k^* and η^*. Analogous to the corresponding motion of a droplet normal to a single plane wall, U/U_0 increases with an increase in k^* for specified values of η^* and a/b and increases with an increase in η^* for fixed values of k^* and a/b.

A careful comparison of Fig. 4 or Table 2 for the case of a slit with Fig. 2 or Table 1 for the case of a single plane wall reveals an interesting feature. When the value of k^* is large,

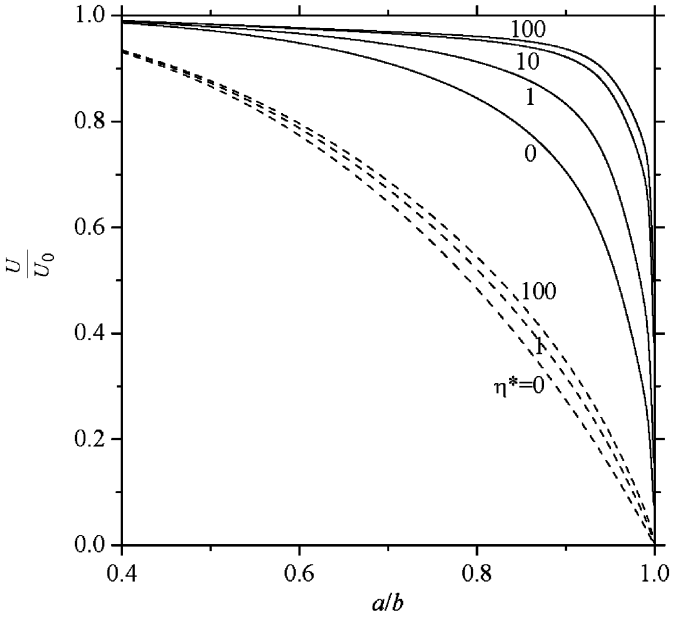

Fig. 4. Plots of the normalized mobility U/U_0 of a spherical droplet situated midway between two parallel plane walls (with $c=b$) undergoing thermocapillary motion perpendicularly versus the separation parameter a/b for several values of η^*. The solid curves represent the case of $k^*=100$ and the dashed curves denote the case of $k^*=0$.

the boundary effect on the thermocapillary motion of a droplet can be weaker for the case of a slit than for the case of a single plane wall with the same value of a/b. Namely, the presence of a second, normal plane wall, even at a symmetric position with respect to the fluid sphere against the first, does not always enhance the wall effect on the thermocapillary migration of the droplet induced by the first plate only. These results reflect the fact that the confining wall can affect the thermal driving force and the viscous drag force on a fluid droplet in opposite directions. Each force is increased in its own direction, but to a different degree, for the case of thermocapillary motion of a droplet in a slit relative to that for the case of migration normal to a single plate. Thus, the net effect composed of these two opposite forces for the slit case is not necessarily to enhance that for the case of a single wall.

In Fig. 5, the collocation results for the normalized mobility U/U_0 of a fluid sphere with $k^*=\eta^*=1$ and $k^*=\eta^*=0$ undergoing thermocapillary motion normal to two plane walls at various positions between them are plotted. The dashed curves (with $a/b=$ constant) illustrate the effect of the position of the second wall (at $z=c$) on the droplet mobility for various values of the relative sphere-to-first-wall spacing b/a. The solid curves (with $2a/(b+c)=$constant) indicate the variation of the droplet mobility as a function of the sphere position at various values of the relative wall-to-wall spacing $(b+c)/2a$. It can be seen that the net wall effect is to reduce the thermocapillary mobility U/U_0 of the droplet. At a constant value of $2a/(b+c)$, the droplet experiences a minimum viscous drag force and has a greatest mobility when it is located midway between the two walls (with $c=b$). The hydrodynamic drag increases and the droplet mobility decreases as the droplet approaches either of

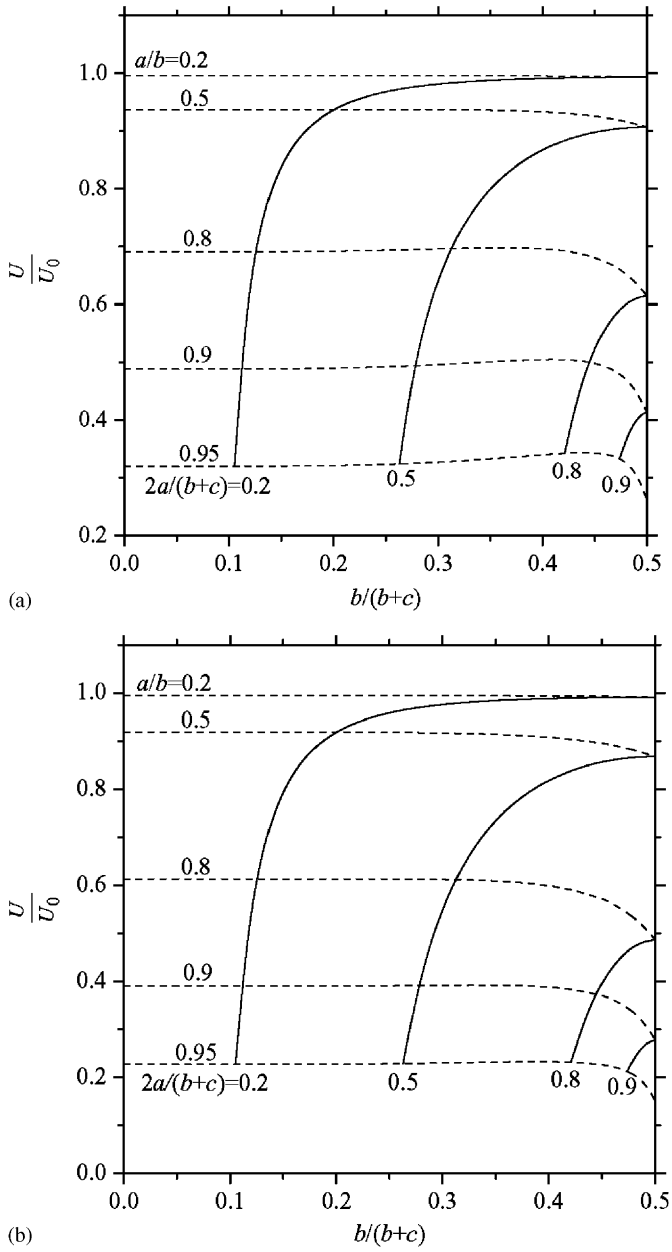

Fig. 5. Plots of the normalized thermocapillary mobility U/U_0 of a spherical droplet migrating perpendicular to two plane walls versus the ratio $b/(b+c)$ with a/b and $2a/(b+c)$ as parameters: (a) for the case $k^*=\eta^*=1$; (b) for the case $k^*=\eta^*=0$.

the walls (or the ratio $b/(b+c)$ decreases). Interestingly, at some specified values of a/b for the droplet undergoing thermocapillary motion near a first wall, the presence and approach of a second plate can increase the velocity of the droplet when it is far from the droplet (c is large), and then reduce the droplet velocity when it is close to the droplet (say, $b/(b+c)>0.4$).

The collocation solution for the problem of sedimentation of a spherical droplet perpendicular to two plane walls at an arbitrary position between them was also obtained recently (Chang and Keh, 2006). Comparing that solution with the present result, we still find that the wall effect on thermocapillary migration in general is much weaker than that on sedimentation. Opposite to the cases of thermocapillary migration illustrated in Fig. 4, the retardation effect on the sedimenting droplet in a slit is stronger for a greater value of η^*.

Since the general problem of thermocapillary motion of a droplet in an arbitrary direction between two parallel plane walls is linear, its solution can be obtained as the vectorial summation of the solutions for its two subproblems: motion perpendicular to the plane walls, which is examined in this paper, and motion parallel to the confining boundaries. The collocation solutions for the thermocapillary motion of a spherical droplet parallel to two plane walls have already been obtained by Keh et al. (2002). It was found that, when the walls are prescribed with a linear temperature profile consistent with the far-field temperature distribution, the wall-corrected normalized thermocapillary migration velocity of the droplet also increases with an increase in k^*. A comparison between Table 3 of Keh et al. and our Table 2 shows that the plane walls in general exert the most influence on the droplet when thermocapillary motion occurs normal to them, and the least in the case of thermocapillary motion parallel to them. Therefore, the direction of thermocapillary motion of a droplet between two parallel plane walls is different from that of the imposed thermal gradient, except when it is oriented parallel or perpendicular to the plane walls.

4. Conclusions

The numerical solution and approximate analytical solution for the quasisteady thermocapillary motion of a spherical droplet perpendicular to two infinite plane walls at an arbitrary position between them have been obtained in this work by using the boundary-collocation technique and the method of reflections, respectively, in the limit of vanishingly small Reynolds and Peclet numbers. It has been found that the boundary effect on thermocapillary motion of a fluid droplet is quite complicated. For specified values of k^* and η^*, the thermocapillary migration velocity of a droplet perpendicular to one or two plane walls is a monotonic decreasing function of the separation parameter a/b. The results of the wall-corrected droplet mobility reflect the dominance of the hydrodynamic retardation exerted by the confining wall on the droplet migration over the possible thermocapillary enhancement due to the thermal interaction between the droplet and the normal walls.

The thermocapillary migration mobility of a spherical droplet parallel to two infinite plane walls at an arbitrary position between them was calculated in a previous work (Keh et al., 2002) for various values of the parameters k^*, η^*, a/b, and $b/(b+c)$. It was found that, for the case of the confining walls prescribed with the far-field temperature profile under the situation of large k^* and η^*, the droplet mobility first decreases with an increase in a/b from $a/b\to 0$ and then increases monotonically from a minimum with further increasing a/b. When the gaps between the droplet and the plane walls turn thin, however, the droplet can even migrate faster than it would as a/b goes to 0 (by as much as 20% for a case of $k^*=\eta^*=100$, $c=b$, and $a/b=0.995$). This interesting feature that U/U_0 may not be a

monotonic function of a/b and can even be greater than unity is understandable because the wall effect of hydrodynamic resistance on the droplet is in competition with the wall effect of thermal enhancement when a droplet with large k^* and η^* is undergoing thermocapillary motion parallel to a plane wall with the imposed far-field temperature distribution. A comparison of this previous work with our results shows that the effect of viscous interactions is stronger or the effect of thermal interactions is weaker in the transverse thermocapillary motion of a fluid sphere in a slit than in the parallel motion. In general, the net boundary effect on thermocapillary motion of a droplet is stronger for the perpendicular migration. For the general problem of a droplet undergoing thermocapillary motion in an arbitrary direction with respect to the two parallel plane walls, the solution can be obtained by adding both the parallel and transverse results vectorially.

Notation

a	radius of the droplet, m
A	thermocapillary mobility defined by Eqs. (1) and (2), $m^2\,s^{-1}\,K^{-1}$
A_n, C_n	coefficients in Eq. (23) for the internal flow field, $m^{-n+3}\,s^{-1}$, $m^{-n+1}\,s^{-1}$
$A(\omega)$, $B(\omega)$, $C(\omega)$, $D(\omega)$	unknown functions in Eq. (21), $m^3\,s^{-1}$
b, c	the respective distances from the droplet center to the two plane walls, m
B	coefficient defined after Eq. (A.8), $m^2\,s^{-1}\,K^{-1}$
B_n, D_n	coefficients in Eq. (22) for the external flow field, $m^{n+2}\,s^{-1}$, $m^n\,s^{-1}$
C, D	dimensionless parameters defined after Eqs. (A.3) and (A.8)
$\mathbf{e}_z$, $\mathbf{e}_r$, $\mathbf{e}_\theta$	unit vectors in z, r, and θ directions
E^2	Stokes operator defined by Eq. (16),m^{-2}
E_∞	$=\lvert\nabla T_\infty\rvert$, $K\,m^{-1}$
G, H	dimensionless parameters defined by Eqs. (A.4) and (A.8)
$G_n^{-1/2}$	Gegenbauer polynomial of the first kind of order n and degree $-\frac{1}{2}$
J_n	Bessel function of the first kind of order n
k	thermal conductivity of the external fluid, $W\,m^{-1}\,K^{-1}$
k_1	thermal conductivity of the droplet, $W\,m^{-1}\,K^{-1}$
k^*	$=k_1/k$
M, N	numbers of collocation points on the droplet surface
P_n	Legendre function of order n
r	radial spherical coordinate, m
R_m, $\overline{R}_m$	coefficients in Eqs. (10)–(12) for the temperature field, m^{m+2}, m^{-m+1}
T	temperature field in the external fluid, K
T_1	temperature field inside the droplet, K
T_0	undisturbed temperature at the droplet center, K
T_∞	prescribed temperature field defined by Eq. (7), K
$\mathbf{U}$, U	droplet velocity, $m\,s^{-1}$
$\mathbf{U}_0$, U_0	velocity of an isolated droplet, $m\,s^{-1}$
v_ρ, v_z	velocity components of the external fluid in cylindrical coordinates, $m\,s^{-1}$
$v_{1\rho}$, v_{1z}	velocity components of the internal fluid in cylindrical coordinates, $m\,s^{-1}$
$X(\omega)$, $Y(\omega)$	unknown functions in Eq. (9), m^3
z	axial cylindrical coordinate, m

Greek letters

$\alpha_{1n}^{(j)}$, $\alpha_{2n}^{(j)}$	functions of r and θ defined by Eqs. (B.4) and (B.5), m^{n-2}, m^n
α_{1n}^*, α_{2n}^*	functions of r and θ defined by Eq. (B.16), m^{n-3}, m^{n-1}
γ	interfacial tension, $kg\,s^{-2}$
$\gamma_{1n}^{(j)}$, $\gamma_{2n}^{(j)}$	functions of r and θ defined by Eqs. (B.6) and (B.7), m^{-n-1}, m^{-n+1}
γ_{1n}^*,γ_{2n}^*	functions of r and θ defined by Eq. (B.17), m^{-n-2}, m^{-n}
$\delta_m^{(1)}$, $\delta_m^{(2)}$, $\delta_m^{(3)}$	functions of r and θ defined by Eqs. (B.1)–(B.3), m^{-m-1}, m^{-m-2}, m^{-m-2}
η_f	viscosity of the fluid droplet, $kg\,m^{-1}\,s^{-1}$
η^*	ratio of viscosities between the internal and external fluids
θ, ϕ	angular spherical coordinates
λ	$=a/b$
ρ	radial cylindrical coordinate, m
$\tau_{r\theta}$, $\tau_{1r\theta}$	viscous shear stresses of the external and internal fluids, $kg\,m^{-1}\,s^{-2}$
Ψ, Ψ_1	Stokes stream functions for the external and internal fluid flows, $m^3\,s^{-1}$

Subscripts

p	droplet
w	wall

Superscript

(i)	the ith reflection

Acknowledgement

This research was partly supported by the National Science Council of the Republic of China.

Appendix A. Analysis of the thermocapillary motion of a fluid sphere normal to one or two plane walls by a method of reflections

In this appendix, the quasisteady thermocapillary migration of a spherical droplet perpendicular either to an infinite plane wall ($c \to \infty$) or to two parallel plane walls with equal distances from the droplet ($c = b$), as shown in Fig. 1, will be

analyzed using a method of reflections. The effect of the walls on the droplet velocity $\mathbf{U}$ is sought in expansions of λ, which equals a/b, the ratio of the droplet radius to the distance between the droplet center and the walls.

A.1. Motion normal to a plane wall

For the problem of thermocapillary migration of a fluid sphere with the relative thermal conductivity k^* and viscosity η^* normal to an infinite plane wall, the governing Eqs. (3) and (14) must be solved by satisfying the boundary conditions (4)–(7) and (17)–(19) with $c \to \infty$. The method-of-reflection solution for the temperature and velocity fields in the external fluid phase consists of the following series, whose terms depend on increasing powers of λ:

$$T = T_0 + E_\infty z + T_p^{(1)} + T_w^{(1)} + T_p^{(2)} + T_w^{(2)} + \cdots, \tag{A.1a}$$

$$\mathbf{v} = \mathbf{v}_p^{(1)} + \mathbf{v}_w^{(1)} + \mathbf{v}_p^{(2)} + \mathbf{v}_w^{(2)} + \cdots, \tag{A.1b}$$

where the subscripts w and p represent the reflections from the wall and the droplet, respectively, and the superscript (i) denotes the ith reflection from that surface. In these series, all the expansion sets of the temperature and velocity fields must satisfy Eqs. (3a) and (14a).

According to Eq. (A.1), the thermocapillary migration velocity of the droplet can also be expressed in the series form

$$\mathbf{U} = U_0\mathbf{e}_z + \mathbf{U}^{(1)} + \mathbf{U}^{(2)} + \cdots. \tag{A.2}$$

In this expression, $U_0 = AE_\infty$ is the thermocapillary migration velocity of an identical droplet in the corresponding unbounded continuous phase given by Eqs. (1) and (2); $\mathbf{U}^{(i)}$ is related to $T_w^{(i)}$ and $\mathbf{v}_w^{(i)}$ by (Anderson, 1985; Chen and Keh, 1990)

$$\mathbf{U}^{(i)} = A[\nabla T_w^{(i)}]_0 + [\mathbf{v}_w^{(i)}]_0 + C\frac{a^2}{6}[\nabla^2\mathbf{v}_w^{(i)}]_0, \tag{A.3}$$

where $C = 3\eta^*(2+3\eta^*)^{-1}$ and the subscript 0 to variables inside brackets denotes evaluation at the position of the droplet center. Note that $0 \leqslant C \leqslant 1$ and the last two terms in Eq. (A.3) represent the Faxen law for the isothermal creeping motion of a freely suspended fluid sphere in the velocity field $\mathbf{v}_w^{(i)}$ (Hetsroni and Haber, 1970).

The solution for the first reflected fields from the droplet is

$$T_p^{(1)} = GE_\infty a^3 r^{-2}\cos\theta, \tag{A.4a}$$

$$\mathbf{v}_p^{(1)} = \tfrac{1}{2}U_0 a^3 r^{-3}(2\cos\theta\mathbf{e}_r + \sin\theta\mathbf{e}_\theta), \tag{A.4b}$$

where $G = (1-k^*)(2+k^*)^{-1}$. Obviously, $-1 \leqslant G \leqslant \frac{1}{2}$, with the upper and lower bounds occurring at the limits $k^* = 0$ and $k^* \to \infty$, respectively. The velocity distribution shown in Eq. (A.4b) is identical to the irrotational flow surrounding a rigid sphere moving with velocity $U_0\mathbf{e}_z$.

The boundary conditions for the ith reflected fields from the wall are derived from Eqs. (6), (7), (18), and (19),

$$z = -b:\ T_w^{(i)} = -T_p^{(i)}, \tag{A.5a}$$

$$\mathbf{v}_w^{(i)} = -\mathbf{v}_p^{(i)}, \tag{A.5b}$$

$$r \to \infty, z > -b:\ T_w^{(i)} \to 0, \tag{A.5c}$$

$$\mathbf{v}_w^{(i)} \to \mathbf{0}. \tag{A.5d}$$

The solution of $T_w^{(i)}$ is obtained by applying Hankel transforms on the variable ρ in Eqs. (3a) and (A.5a,c) (taking $i=1$), with the result

$$T_w^{(1)} = GE_\infty a^3(2b+z)[\rho^2 + (2b+z)^2]^{-3/2}. \tag{A.6a}$$

This reflected temperature field may be interpreted as arising from the reflection of the imposed field $E_\infty\mathbf{e}_z$ from a fictitious droplet identical to the actual droplet, its location being at the mirror-image position of the actual droplet with respect to the plane $z=-b$ (i.e., at $x=0$, $y=0$, $z=-2b$). The solution of $\mathbf{v}_w^{(1)}$ can also be obtained by applying Hankel transforms to the Stokes (14a) twice and to the boundary conditions (A.5b, d), which results in

$$\mathbf{v}_w^{(1)} = -\frac{1}{2}U_0 a^3\int_0^\infty \omega^2[E(\omega,z)J_1(\omega\rho)\mathbf{e}_\rho + F(\omega,z)J_0(\omega\rho)\mathbf{e}_z]\,\mathrm{d}\omega, \tag{A.6b}$$

where

$$E(\omega,z) = [2(b+z)\omega - 1]\mathrm{e}^{-\omega(z+2b)},$$

$$F(\omega,z) = [2(b+z)\omega + 1]\mathrm{e}^{-\omega(z+2b)}.$$

The contributions of $T_w^{(1)}$ and $\mathbf{v}_w^{(1)}$ to the droplet velocity are determined using Eq. (A.3),

$$\mathbf{U}_t^{(1)} = A[\nabla T_w^{(1)}]_{r=0} = -\tfrac{1}{4}G\lambda^3 U_0\mathbf{e}_z, \tag{A.7a}$$

$$\mathbf{U}_h^{(1)} = \left[\mathbf{v}_w^{(1)} + C\frac{a^2}{6}\nabla^2\mathbf{v}_w^{(1)}\right]_{r=0} = -\frac{1}{4}(2\lambda^3 - C\lambda^5)U_0\mathbf{e}_z, \tag{A.7b}$$

$$\mathbf{U}^{(1)} = \mathbf{U}_t^{(1)} + \mathbf{U}_h^{(1)} = \tfrac{1}{4}[-(2+G)\lambda^3 + C\lambda^5]U_0\mathbf{e}_z. \tag{A.7c}$$

Eq. (A.7a) shows that the reflected temperature field from the plane wall can decrease (if $G>0$ or $k^*<1$) or increase (if $G<0$ or $k^*>1$) the migration velocity of the droplet from its undisturbed value, while Eq. (A.7b) indicates that the reflected velocity field is to decrease this velocity; the net effect of the reflected fields is expressed by Eq. (A.7c), which always retards the movement of the droplet, irrespective of the values of G (or k^*), η^*, and λ. When $G=0$ (or $k^*=1$), the reflected temperature field makes no contribution to the thermocapillary migration velocity. For any given values of η^* and λ, the normalized droplet velocity increases monotonically with an increase

in k^*. Eq. (A.7) indicates that the wall correction to the velocity of the thermocapillary droplet is $O(\lambda^3)$, which is weaker than that obtained for the corresponding sedimentation problem, in which the leading boundary effect is $O(\lambda)$. Note that the wall effect on thermocapillary motion involving the viscosity parameter η^* appears starting from $O(\lambda^5)$, and the normalized droplet velocity increases with an increase in η^*.

The solution for the second reflected fields from the droplet is

$$T_p^{(2)} = E_\infty[-\tfrac{1}{4}G^2\lambda^3a^3r^{-2}\cos\theta + \tfrac{1}{16}GH\lambda^4a^4r^{-3} \times (3\cos^2\theta - 1) + O(\lambda^5a^5)], \tag{A.8a}$$

$$\mathbf{v}_p^{(2)} = U_0\left\{-\frac{1}{8}G\lambda^3a^3r^{-3}(2\cos\theta\mathbf{e}_r + \sin\theta\mathbf{e}_\theta) - \frac{3}{64} \times \left(D + 2G\frac{B}{A}\right)\lambda^4a^2r^{-2}(3\cos^2\theta - 1)\mathbf{e}_r + \frac{3}{32}G\frac{B}{A} \times \lambda^4a^4r^{-4}[(3\cos^2\theta - 1)\mathbf{e}_r + 2\sin\theta\cos\theta\mathbf{e}_\theta]\right\}, \tag{A.8b}$$

where $H = 3(1-k^*)(3+2k^*)^{-1}$, $B = 3(3+2k^*)^{-1}(1+\eta^*)^{-1}(-\partial\gamma/\partial T)(a/\eta_f)$, and $D = 3(2+5\eta^*)(1+\eta^*)^{-1}$.

The boundary conditions for the second reflected fields from the wall are obtained by substituting the results of $T_p^{(2)}$ and $\mathbf{v}_p^{(2)}$ into Eq. (A.5), with which Eqs. (3a) and (14a) can be solved as before to yield

$$[\nabla T_w^{(2)}]_{r=0} = \tfrac{1}{256}E_\infty[16G^2\lambda^6 + 6GH\lambda^8 + O(\lambda^9)]\mathbf{e}_z, \tag{A.9a}$$

$$\left[\mathbf{v}_w^{(2)} + C\frac{a^2}{6}\nabla^2\mathbf{v}_w^{(2)}\right]_{r=0} = U_0\left\{\frac{1}{256}\left[32G - 9\left(D + 2G\frac{B}{A}\right)\right]\lambda^6 + \frac{1}{512}\left[-32GC + 9\left(D + 2G\frac{B}{A}\right)C\right]\lambda^8 + O(\lambda^9)\right\}\mathbf{e}_z. \tag{A.9b}$$

The contribution of the second reflected fields to the droplet velocity is obtained by combining Eqs. (A.3) and (A.9), which gives

$$\mathbf{U}^{(2)} = U_0\left\{\frac{1}{256}\left[-9\left(D + 2G\frac{B}{A}\right) + 16(2+G)G\right]\lambda^6 + \frac{1}{512}\left[9\left(D + 2G\frac{B}{A}\right)C + 4(3H - 8C)G\right]\lambda^8 + O(\lambda^9)\right\}\mathbf{e}_z. \tag{A.10}$$

Obviously, $\mathbf{U}^{(3)}$ will be $O(\lambda^9)$. With the substitution of Eqs. (A.7c) and (A.10) into Eq. (A.2), the droplet velocity can be expressed as $\mathbf{U} = U\mathbf{e}_z$ with

$$U = U_0\left\{1 - \frac{1}{4}(2+G)\lambda^3 + \frac{1}{4}C\lambda^5 - \frac{1}{256}\left[9\left(D + 2G\frac{B}{A}\right) - 16(2+G)G\right]\lambda^6 + \frac{1}{512}\left[9\left(D + 2G\frac{B}{A}\right)C + 4(3H - 8C)G\right]\lambda^8 + O(\lambda^9)\right\}. \tag{A.11}$$

Owing to the linearity of the problem, the above analysis is valid when the droplet is either approaching the plane wall or receding from it.

A.2. Motion normal to two parallel plane walls

For the problem of thermocapillary migration of a spherical droplet perpendicular to two infinite plane walls with equal distances from the droplet, the boundary conditions corresponding to governing Eqs. (3) and (14) are given by Eqs. (4)–(7) and (17)–(19) with $c = b$. With $\lambda = a/b \ll 1$, the series expansions of the temperature, fluid velocity, and droplet velocity given by Eqs. (A.1), (A.2), and (A.4) remain valid here. From Eqs. (5)–(7), (18), and (19), the boundary conditions for $T_w^{(i)}$ and $\mathbf{v}_w^{(i)}$ are found to be

$$|z| = b:\ T_w^{(i)} = -T_p^{(i)}, \tag{A.12a}$$

$$\mathbf{v}_w^{(i)} = -\mathbf{v}_p^{(i)}, \tag{A.12b}$$

$$r \to \infty,\ |z| \leqslant b:\ T_w^{(i)} \to 0, \tag{A.12c}$$

$$\mathbf{v}_w^{(i)} \to \mathbf{0}. \tag{A.12d}$$

The first wall-reflected fields can be solved by the same method as used for the case of a single plane wall in the previous subsection, with the result

$$T_w^{(1)} = -GE_\infty a\lambda^2\int_0^\infty \frac{1+e^{-2\alpha}}{\sinh(2\alpha)}\sinh\left(\frac{\alpha}{b}z\right) \times \alpha J_0\left(\frac{\alpha}{b}\rho\right)d\alpha, \tag{A.13a}$$

$$\mathbf{v}_w^{(1)} = -\frac{1}{2}U_0\lambda^3\int_0^\infty \alpha^2\left[E(\alpha,z)J_1\left(\frac{\alpha}{b}\rho\right)\mathbf{e}_\rho + F(\alpha,z)J_0\left(\frac{\alpha}{b}\rho\right)\mathbf{e}_z\right]d\alpha, \tag{A.13b}$$

where

$$E(\alpha,z) = \frac{2}{2\alpha + \sinh(2\alpha)}\left[(1 - \alpha - e^{-\alpha}\sinh\alpha)\sinh\left(\frac{\alpha}{b}z\right) + \frac{\alpha}{b}z\cosh\left(\frac{\alpha}{b}z\right)\right], \tag{A.14a}$$

$$F(\alpha,z) = \frac{2}{2\alpha + \sinh(2\alpha)}\left[(\alpha + e^{-\alpha}\sinh\alpha)\cosh\left(\frac{\alpha}{b}z\right) - \frac{\alpha}{b}z\sinh\left(\frac{\alpha}{b}z\right)\right]. \tag{A.14b}$$

The contributions of $T_w^{(1)}$ and $\mathbf{v}_w^{(1)}$ to the droplet velocity are determined using Eq. (A.3), which lead to a result similar to Eq. (A.7),

$$\mathbf{U}_t^{(1)} = A[\nabla T_w^{(1)}]_{r=0} = -d_1 G\lambda^3 U_0 \mathbf{e}_z, \tag{A.15a}$$

$$\mathbf{U}_h^{(1)} = \left[\mathbf{v}_w^{(1)} + \frac{a^2}{6} C\nabla^2 \mathbf{v}_w^{(1)}\right]_{r=0} = [-d_2\lambda^3 + d_3 C\lambda^5] U_0 \mathbf{e}_z, \tag{A.15b}$$

$$\mathbf{U}^{(1)} = \mathbf{U}_t^{(1)} + \mathbf{U}_h^{(1)} = [-(d_2 + d_1 G)\lambda^3 + d_3 C\lambda^5] U_0 \mathbf{e}_z, \tag{A.15c}$$

where

$$d_1 = \int_0^\infty \frac{1 + \mathrm{e}^{-2\alpha}}{\sinh(2\alpha)} \alpha^2 \,\mathrm{d}\alpha = 0.60103, \tag{A.16a}$$

$$d_2 = \int_0^\infty \frac{\sinh(\alpha)\mathrm{e}^{-\alpha} + \alpha}{2\alpha + \sinh(2\alpha)} \alpha^2 \,\mathrm{d}\alpha = 0.79076, \tag{A.16b}$$

$$d_3 = \frac{1}{3} \int_0^\infty \frac{\alpha^4}{2\alpha + \sinh(2\alpha)} \,\mathrm{d}\alpha = 0.44175. \tag{A.16c}$$

Again, Eq. (A.15a) shows that the reflected temperature field from the confining walls can decrease (if $G > 0$ or $k^* < 1$) or increase (if $G < 0$ or $k^* > 1$) the droplet velocity, while Eq. (A.15b) indicates that the reflected velocity field is to decrease this velocity; the net effect is expressed by Eq. (A.15c), which can enhance or retard the movement of the droplet, depending on the combination of the values of G (or k^*), η^*, and λ. Note that, when the value of η^* is large, the necessary condition for the wall enhancement on the thermocapillary motion to occur is a large value of k^* and a value of λ close to unity such that the relation $d_3 C\lambda^5 > (d_2 + d_1 G)\lambda^3$ is warranted.

Analogous to the previous case, the results of the second reflections can be obtained as

$$T_p^{(2)} = -E_\infty [d_1 G^2 \lambda^3 a^3 r^{-2} \cos\theta + O(\lambda^5 a^5)], \tag{A.17a}$$

$$\mathbf{v}_p^{(2)} = -\tfrac{1}{2} U_0 d_1 G\lambda^3 a^3 r^{-3} (2\cos\theta \mathbf{e}_r + \sin\theta \mathbf{e}_\theta) + O(\lambda^5 a^3), \tag{A.17b}$$

$$[\nabla T_w^{(2)}]_{r=0} = E_\infty [d_1^2 G^2 \lambda^6 + O(\lambda^9)] \mathbf{e}_z, \tag{A.18a}$$

$$\left[\nabla \mathbf{v}_w^{(2)} + \frac{a^2}{6} C\nabla^2 \mathbf{v}_w^{(2)}\right]_{r=0} = U_0 [d_1 d_2 G\lambda^6 - d_1 d_3 CG\lambda^8 + O(\lambda^9)] \mathbf{e}_z, \tag{A.18b}$$

and

$$\mathbf{U}^{(2)} = [(d_1^2 G^2 + d_1 d_2 G)\lambda^6 - d_1 d_3 CG\lambda^8 + O(\lambda^9)] U_0 \mathbf{e}_z. \tag{A.19}$$

Note that the $\lambda^4 a^2$ and $\lambda^4 a^4$ terms in the expressions for $T_p^{(2)}$ and $\mathbf{v}_p^{(2)}$ vanish.

With the combination of Eqs. (A.2), (A.15c), and (A.19), the droplet velocity can be expressed as $\mathbf{U} = U\mathbf{e}_z$ with

$$U = U_0 [1 - (d_2 + d_1 G)\lambda^3 + d_3 C\lambda^5 + (d_1^2 G^2 + d_1 d_2 G)\lambda^6 - d_1 d_3 CG\lambda^8 + O(\lambda^9)]. \tag{A.20}$$

This result is valid for a droplet undergoing thermocapillary motion toward either of the two plane walls.

Comparing Eq. (A.20) for the slit case with Eq. (A.11) for the case of a single normal plane, one can find that the wall effects on the thermocapillary motion of a droplet in the two cases are qualitatively similar. However, the assumption that the result of the boundary effect for two walls can be obtained by simple addition of the single-wall effect generally gives a greater correction to thermocapillary motion, similar to the case of the corresponding sedimentation problem (Happel and Brenner, 1983).

Appendix B. Definitions of some functions in Section 2

The functions $\delta_m^{(1)}$, $\delta_m^{(2)}$, and $\delta_m^{(3)}$ in Eqs. (12), (13), and (26d) are defined by

$$\delta_m^{(1)}(r,\theta) = \int_0^\infty \omega[-B_{1m}''(\omega,-b)\sinh\eta + B_{1m}''(\omega,c)\sinh\sigma] \times (\sinh^{-1}\tau) J_0(\omega r\sin\theta)\,\mathrm{d}\omega + r^{-m-1} P_m(\cos\theta), \tag{B.1}$$

$$\delta_m^{(2)}(r,\theta) = \int_0^\infty \omega^2 \{\sin\theta [B_{1m}''(\omega,-b)\sinh\eta - B_{1m}''(\omega,c)\sinh\sigma] J_1(r\omega\sin\theta) + \cos\theta \times [-B_{1m}''(\omega,-b)\cosh\eta + B_{1m}''(\omega,c)\cosh\sigma] \times J_0(r\omega\sin\theta)\}(\sinh^{-1}\tau)\,\mathrm{d}\omega - (m+1) r^{-m-2} P_m(\cos\theta), \tag{B.2}$$

$$\delta_m^{(3)}(r,\theta) = \int_0^\infty \omega^2 \{\cos\theta [B_{1m}''(\omega,-b)\sinh\eta - B_{1m}''(\omega,c)\sinh\sigma] J_1(r\omega\sin\theta) + \sin\theta \times [B_{1m}''(\omega,-b)\cosh\eta - B_{1m}''(\omega,c)\cosh\sigma] \times J_0(r\omega\sin\theta)\}(\sinh^{-1}\tau)\,\mathrm{d}\omega + m r^{-m-2} \times [P_m(\cos\theta)\cos\theta - P_{m-1}(\cos\theta)]\csc\theta, \tag{B.3}$$

and the functions $\alpha_{in}^{(j)}$ and $\gamma_{in}^{(j)}$ for i and j equal to 1 or 2 in Eqs. (24)–(26) are defined by

$$\alpha_{in}^{(1)}(r,\theta) = -r^{n+2i-4}[(n+1)G_{n+1}^{-1/2}(\cos\theta)\csc\theta - (2n+2i-3)G_n^{-1/2}(\cos\theta)\cot\theta], \tag{B.4}$$

$$\alpha_{in}^{(2)}(r,\theta) = -r^{n+2i-4}[(2n+2i-3)G_n^{-1/2}(\cos\theta) + P_n(\cos\theta)], \tag{B.5}$$

$$\gamma_{in}^{(1)}(r,\theta) = -\int_0^\infty [G_+''(\sigma,\eta)B_{in}'(\omega,-b) - G_+''(\eta,\sigma)B_{in}'(\omega,c) - G_+'(\sigma,\eta)B_{in}''(\omega,-b) + G_+'(\eta,\sigma)B_{in}''(\omega,c)] \times \omega J_1(\omega r\sin\theta)\mathrm{d}\omega - r^{-n+2i-3}[(n+1)G_{n+1}^{-1/2} \times (\cos\theta\csc\theta - 2(i-1)G_n^{-1/2}(\cos\theta)\cot\theta], \tag{B.6}$$

$$\gamma_{in}^{(2)}(r,\theta)=-\int_0^\infty [-G'_-(\sigma,\eta)B'_{in}(\omega,-b)+G'_-(\eta,\sigma)B'_{in}(\omega,c) + G''_-(\sigma,\eta)B''_{in}(\omega,-b) - G''_-(\eta,\sigma)B''_{in}(\omega,c)] \times \omega J_0(\omega r\sin\theta)\,\mathrm{d}\omega - r^{-n+2i-3}[P_n(\cos\theta) + 2(i-1)G_n^{-1/2}(\cos\theta)], \tag{B.7}$$

where

$$B'_{1n}(\omega,z)=-\frac{1}{n!}\left(\frac{\omega|z|}{z}\right)^{n-1}\mathrm{e}^{-\omega|z|}, \tag{B.8}$$

$$B''_{1n}(\omega,z)=-\frac{\omega^{n-1}}{n!}\left(\frac{|z|}{z}\right)^{n}\mathrm{e}^{-\omega|z|}, \tag{B.9}$$

$$B'_{2n}(\omega,z)= -\frac{1}{n!}\left(\frac{\omega|z|}{z}\right)^{n-3}[(2n-3)\omega|z| - n(n-2)]\mathrm{e}^{-\omega|z|}, \tag{B.10}$$

$$B''_{2n}(\omega,z)= -\frac{\omega^{n-3}}{n!}\left(\frac{|z|}{z}\right)^{n}[(2n-3)\omega|z| - (n-1)(n-3)]\mathrm{e}^{-\omega|z|}, \tag{B.11}$$

$$G'_{\pm}(\mu,\nu)=\tau^*\mu\nu(\mu'\pm\tau'\nu'), \tag{B.12}$$

$$G''_{\pm}(\mu,\nu)=\tau^*[\nu(\cosh\mu-\tau'\nu')\pm\mu(\mu'-\tau'\cosh\nu)], \tag{B.13}$$

$$\mu'=\frac{\sinh\mu}{\mu},\quad \nu'=\frac{\sinh\nu}{\nu},\quad \tau'=\frac{\sinh\tau}{\tau},$$

$$\tau^*=\frac{\tau}{\sinh^2\tau-\tau^2}, \tag{B.14}$$

$$\sigma=\omega(r\cos\theta+b),\quad \eta=\omega(r\cos\theta-c),$$

$$\tau=\omega(b+c). \tag{B.15}$$

The functions α^*_{in} and γ^*_{in} for i equal to 1 or 2 in Eq. (26d) is defined by

$$\alpha^*_{in}(r,\theta)= -r^{n+2i-5}[(n+1)(n+2i-5)G_{n+1}^{-1/2}(\cos\theta)\cot\theta - (n+2i-5)(2n+2i-3)G_n^{-1/2}(\cos\theta)\csc\theta + (5-2i+n\cot^2\theta)P_n(\cos\theta)\sin\theta - nP_{n-1}(\cos\theta)\cot\theta], \tag{B.16}$$

$$\gamma^*_{in}(r,\theta)= -\cos\theta\sin\theta[C^*_{in}(r,\theta)+D^*_{in}(r,\theta)] - (\cos^2\theta-\sin^2\theta)[C^{**}_{in}(r,\theta)+D^{**}_{in}(r,\theta)], \tag{B.17}$$

where

$$C^*_{1n}(r,\theta)= -2r^{-(n+2)}[(n+1)(n+\csc^2\theta)G_{n+1}^{-1/2}(\cos\theta) - (3n+2)P_n(\cos\theta)\cos\theta + nP_{n-1}(\cos\theta)], \tag{B.18}$$

$$C^*_{2n}(r,\theta)=2r^{-n}[2(2n-1+\cot^2\theta)G_n^{-1/2}(\cos\theta)\cos\theta - (n+1)(n-1+\cot^2\theta)G_{n+1}^{-1/2}(\cos\theta) - (n+2-4\sin^2\theta)P_{n-1}(\cos\theta) + 3nP_n(\cos\theta)\cos\theta], \tag{B.19}$$

$$C^{**}_{1n}(r,\theta)= -r^{-(n+2)}\{n\cot\theta[(n+1)G_{n+1}^{-1/2}(\cos\theta) + P_{n-1}(\cos\theta)] + [(3n+2)\sin\theta - n\csc\theta] \times P_n(\cos\theta)\}, \tag{B.20}$$

$$C^{**}_{2n}(r,\theta)= -r^{-n}\{2[2(n-1)\sin\theta-(n-2)\csc\theta] \times G_n^{-1/2}(\cos\theta) + (n^2-n-2)G_{n+1}^{-1/2}(\cos\theta)\cot\theta + (n-4\sin^2\theta)P_{n-1}(\cos\theta)\cot\theta + n(3\sin\theta-\csc\theta)P_n(\cos\theta)\}, \tag{B.21}$$

$$D^*_{in}(r,\theta)=\int_0^\infty\{[G''_+(\sigma,\eta)B'_{in}(\omega,-b)-G''_+(\eta,\sigma)B'_{in}(\omega,c) - G'_+(\sigma,\eta)B''_{in}(\omega,-b)+G'_+(\eta,\sigma)B''_{in}(\omega,c)] \times [J_0(\omega r\sin\theta)-J_2(\omega r\sin\theta)] + 2[G^*_-(\sigma,\eta)B'_{in}(\omega,-b)-G^*_-(\eta,\sigma)B'_{in}(\omega,c) - G^{**}_-(\sigma,\eta)B''_{in}(\omega,-b)+G^{**}_-(\eta,\sigma)B''_{in}(\omega,c)] \times J_0(\omega r\sin\theta)\}\omega^2\,\mathrm{d}\omega, \tag{B.22}$$

$$D^{**}_{in}(r,\theta)=\int_0^\infty\{[G^{**}_+(\sigma,\eta)B'_{in}(\omega,-b)-G^{**}_+(\eta,\sigma)B'_{in}(\omega,c) - G^*_+(\sigma,\eta)B''_{in}(\omega,-b)+G^*_+(\eta,\sigma)B''_{in}(\omega,c)] + [G'_-(\sigma,\eta)B'_{in}(\omega,-b)-G'_-(\eta,\sigma)B'_{in}(\omega,c) - G''_-(\sigma,\eta)B''_{in}(\omega,-b)+G''_-(\eta,\sigma)B''_{in}(\omega,c)]\} \times \omega^2 J_1(\omega r\sin\theta)\,\mathrm{d}\omega, \tag{B.23}$$

and

$$G^*_{\pm}(\mu,\nu)=\tau^*[(\mu+\nu)(\mu'\pm\tau'\nu')+\nu(\cosh\mu-\mu') \pm\tau'\mu(\cosh\nu-\nu')], \tag{B.24}$$

$$G^{**}_{\pm}(\mu,\nu)=\tau^*[\cosh\mu-\tau'\nu'\pm(\mu'-\tau'\cosh\nu) + \nu\sinh\mu-\tau'(\cosh\nu-\nu') \pm(\cosh\mu-\mu'-\tau'\mu\sinh\nu)]. \tag{B.25}$$

References

Anderson, J.L., 1985. Droplet interactions in thermocapillary motion. International Journal of Multiphase Flow 11, 813–824.

Ascoli, E.P., Leal, L.G., 1990. Thermocapillary motion of a deformable drop toward a planar wall. Journal of Colloid and Interface Science 138, 220–230.

Barton, K.D., Subramanian, R.S., 1990. Thermocapillary migration of a liquid drop normal to a plane surface. Journal of Colloid and Interface Science 137, 170–182.

Barton, K.D., Subramanian, R.S., 1991. Migration of liquid drops in a vertical temperature gradient—interaction effects near a horizontal surface. Journal of Colloid and Interface Science 141, 146–156.

Berejnov, V., Lavrenteva, O.M., Nir, A., 2001. Interaction of two deformable viscous drops under external temperature gradient. Journal of Colloid and Interface Science 242, 202–213.

Chang, Y.C., Keh, H.J., 2006. Slow motion of a slip spherical particle perpendicular to two plane walls. Journal of Fluids and Structures, in press.

Chen, S.H., Keh, H.J., 1990. Thermocapillary motion of a fluid droplet normal to a plane surface. Journal of Colloid and Interface Science 137, 550–562.

Chen, J., Dagan, Z., Maldarelli, C., 1991. The axisymmetric thermocapillary motion of a fluid particle in a tube. Journal of Fluid Mechanics 233, 405–437.

Ganatos, P., Weinbaum, S., Pfeffer, R., 1980. A strong interaction theory for the creeping motion of a sphere between plane parallel boundaries. Part 1. Perpendicular motion. Journal of Fluid Mechanics 99, 739–753.

Happel, J., Brenner, H., 1983. Low Reynolds Number Hydrodynamics. Nijhoff, The Hague, The Netherlands.

Hetsroni, G., Haber, S., 1970. The flow in and around a droplet or bubble submerged in an unbound arbitrary velocity field. Rheological Acta 9, 488–496.

Kasumi, H., Solomentsev, Y.E., Guelcher, S.A., Anderson, J.L., Sides, P.J., 2000. Thermocapillary flow and aggregation of bubbles on a solid wall. Journal of Colloid and Interface Science 232, 111–120.

Keh, H.J., Chen, S.H., 1990. The axisymmetric thermocapillary motion of two fluid droplets. International Journal of Multiphase Flow 16, 515–527.

Keh, H.J., Chen, L.S., 1992. Droplet interactions in axisymmetric thermocapillary motion. Journal of Colloid and Interface Science 151, 1–16.

Keh, H.J., Chen, L.S., 1993. Droplet interactions in thermocapillary migration. Chemical Engineering Science 48, 3565–3582.

Keh, H.J., Lien, L.C., 1991. Electrophoresis of a colloidal sphere along the axis of a circular orifice or a circular disk. Journal of Fluid Mechanics 224, 305–333.

Keh, H.J., Chen, P.Y., Chen, L.S., 2002. Thermocapillary motion of a fluid droplet parallel to two plane walls. International Journal of Multiphase Flow 28, 1149–1175.

Loewenberg, M., Davis, R.H., 1993. Near-contact, thermocapillary migration of a nonconducting, viscous drop normal to a planar interface. Journal of Colloid and Interface Science 160, 265–274.

Meyyappan, M., Subramanian, R.S., 1987. Thermocapillary migration of a gas bubble in an arbitrary direction with respect to a plane surface. Journal of Colloid and Interface Science 115, 206–219.

Meyyappan, M., Wilcox, W.R., Subramanian, R.S., 1981. Thermocapillary migration of a bubble normal to a plane surface. Journal of Colloid and Interface Science 83, 199–208.

Morton, D.S., Subramanian, R.S., Balasubramaniam, R., 1990. The migration of a compound drop due to thermocapillarity. Physics of Fluids A 2, 2119–2133.

Sadhal, S.S., 1983. A note on the thermocapillary migration of a bubble normal to a plane surface. Journal of Colloid and Interface Science 95, 283–285.

Sellier, A., 2005. Thermocapillary motion of a two-bubble cluster near a plane solid wall. Comptes Rendus Mecanique 333, 636–641.

Sun, R., Hu, W.R., 2003. Planar thermocapillary migration of two bubbles in microgravity environment. Physics of Fluids 15, 3015–3027.

Young, N.O., Goldstein, J.S., Block, M.J., 1959. The motion of bubbles in a vertical temperature gradient. Journal of Fluid Mechanics 6, 350–364.